

See discussions, stats, and author profiles for this publication at: <https://www.researchgate.net/publication/226994990>

Determination of the oxidation state of radiogenic Pb in natural zircon using X-ray absorption near-edge structure

ARTICLE *in* PHYSICS AND CHEMISTRY OF MINERALS · APRIL 2010

Impact Factor: 1.54 · DOI: 10.1007/s00269-009-0330-2

CITATIONS

3

READS

31

5 AUTHORS, INCLUDING:



Kazuya Tanaka

Japan Atomic Energy Agency

51 PUBLICATIONS 596 CITATIONS

SEE PROFILE



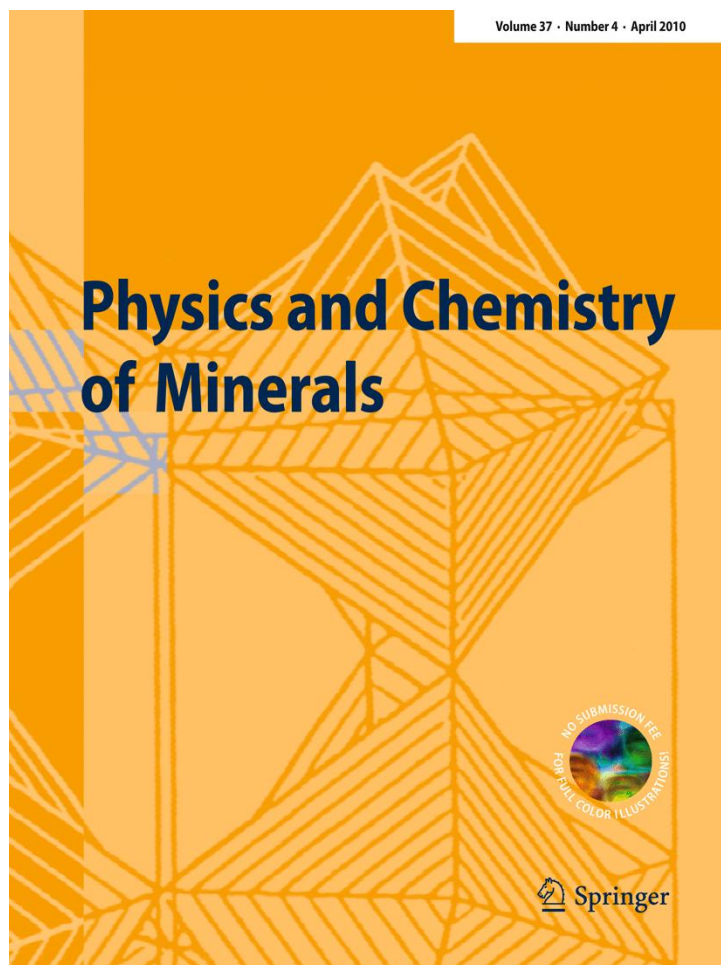
Kenji Horie

National Institute of Polar Research

81 PUBLICATIONS 707 CITATIONS

SEE PROFILE

ISSN 0342-1791, Volume 37, Number 4



**This article was published in the above mentioned Springer issue.
The material, including all portions thereof, is protected by copyright;
all rights are held exclusively by Springer Science + Business Media.**

**The material is for personal use only;
commercial use is not permitted.**

**Unauthorized reproduction, transfer and/or use
may be a violation of criminal as well as civil law.**

Determination of the oxidation state of radiogenic Pb in natural zircon using X-ray absorption near-edge structure

Kazuya Tanaka · Yoshio Takahashi ·
Kenji Horie · Hiroshi Shimizu · Takashi Murakami

Received: 31 May 2009 / Accepted: 10 September 2009 / Published online: 14 March 2010
© Springer-Verlag 2010

Abstract We examined the L_{III}-edge Pb X-ray absorption near-edge structure (XANES) of three natural zircon samples with different amounts of radiation doses (1.9×10^{15} to 6.8×10^{15} α -decay events/mg). The results suggest that the oxidation state of radiogenic Pb in the zircon sample with the highest radiation dose is divalent. The XANES spectra of the two other samples with lower radiation doses suggest that radiogenic Pb(II) is present, and further that some Pb may be tetravalent. This is the first work on the determination of the oxidation state of radiogenic Pb in natural zircon using XANES.

Keywords Oxidation state · Radiogenic Pb · XANES · Zircon

Introduction

Zircon (ZrSiO₄) occurs as a common accessory mineral in rocks. Because zircon typically contains U, Th and a small quantity of Pb (initially incorporated into zircon as common Pb), zircon has been used for dating based on the U–Th–Pb systematics to determine the geological time scale (Faure 1986). Despite zircon is durable against chemical weathering, its crystal structure and physical properties are modified due to radiation damage caused by α -recoil during the radioactive decays of the ²³⁸U, ²³⁵U, and ²³²Th series (e.g. Murakami et al. 1991; Utsunomiya et al. 2007). The crystal structure changes from a crystalline to an aperiodic and metamict state with increasing radiation doses. Such a structural change due to radiation damage has also been experimentally investigated by heavy-ion beam irradiation on zircon (Meldrum et al. 1998; Zhang et al. 2008). Davis and Krogh (2000) suggested that radiogenic Pb is preferentially leached from α -recoil-damaged lattice sites in zircon.

The coordination environment of radiogenic Pb in zircon is fundamental information to understand the disturbance of the Pb isotope system. In a number of studies, several researchers have proved that X-ray absorption fine structure (XAFS) spectroscopy is useful for the speciation of trace elements in natural samples (Reeder et al. 1999; Kelley et al. 2003; Takahashi et al. 2007a, b). In XAFS, there are two energy regions: an X-ray absorption near-edge structure (XANES) and extended X-ray absorption fine structure (EXAFS). EXAFS provides the local coordination structure of a given atom, including the coordination number and distance from neighboring atoms. Reeder et al. (1999) reported the local coordination structure of Pb²⁺ in natural calcite with 735 ppm Pb using EXAFS. Takahashi et al. (2007a) measured the EXAFS

K. Tanaka · Y. Takahashi · H. Shimizu
Department of Earth and Planetary Systems Sciences,
Graduate School of Science, Hiroshima University,
Higashi-Hiroshima, Hiroshima 739-8526, Japan

K. Horie
Geological Survey of Japan, National Institute of Advanced
Industrial Science and Technology, AIST Tsukuba Central 7,
Tsukuba 305-8567, Japan

T. Murakami
Department of Earth and Planetary Science,
The University of Tokyo, 7-3-1 Hongo,
Tokyo 113-0033, Japan

Present Address:

K. Tanaka (✉)
Advanced Science Research Center, Japan Atomic Energy
Agency, Tokai, Ibaraki 319-1195, Japan
e-mail: tanaka.kazuya24@jaea.go.jp

spectra of ferromanganese nodules with 1,600–1,900 ppm Pb. The quantity of Pb in natural zircon is unfortunately too low for the successful application of EXAFS. However, the XANES spectrum of Pb in natural zircon, which provides its oxidation state, can be recorded using the fluorescence method with a multi-element semiconductor Ge detector (SSD). The introduction of SSD into the XAFS measurement improved the sensitivity, which in turn made it possible to apply XAFS to the speciation of trace elements in natural samples (e.g. Reeder et al. 1999; Takahashi et al. 2007a, b). In particular, Takahashi et al. (2007b) successfully determined the speciation of radiogenic Os produced by the radioactive decay of Re in molybdenite.

The main objective of this study is to determine the oxidation state of radiogenic Pb in natural zircon. The oxidation state of Pb in natural and synthetic zircon has often been discussed (e.g. Watson et al. 1997; Utsunomiya et al. 2004), but it has not been determined using a direct method such as XANES. Since the ionic size of Pb(II) (1.18 Å, CN6) is much larger than that of Pb(IV) (0.775 Å, CN6) (Shannon 1976), the determination of the oxidation state of Pb in natural zircon will contribute to inferring its compatibility in the zircon structure, even if EXAFS is unavailable in the present work.

Samples and XANES measurement

Three natural zircon samples (4102, 4302 and 4603), obtained in Sri Lanka, were used for XANES analysis (Murakami et al. 1991). Each sample is a large single crystal, with the longest dimension 5–10 mm. The average age of these samples is 570 ± 20 Ma (Gottfried et al. 1956). The structures of these samples with different radiation doses and therefore with different α -decay event damages were well investigated by Murakami et al. (1991). Evidence for metamorphic deformation or chemical alteration was not observed. The samples have different U and Th concentrations, which results in the accumulation of different amounts of radiogenic Pb (Table 1). The radiogenic Pb concentrations of the zircon samples were calculated from the U and Th concentrations and the average age of the samples (i.e. 570 Ma). The calculations were based on the following equations: $D = P_0 - P$ and

$P = P_0 \exp(-\lambda t)$ (P_0 initial parent nuclide, P present parent nuclide, D present daughter nuclide, λ decay constant, t age). The amounts of daughter nuclides were calculated for the ^{238}U , ^{235}U , and ^{232}Th series. Because these samples have zoning structures, the U and Th concentrations of each sample shown in Table 1 are average values of all zones of each sample (Murakami et al. 1991). Therefore, the calculated radiogenic Pb concentrations also are the average ones. Although Pb has four stable isotopes of ^{204}Pb , ^{206}Pb , ^{207}Pb and ^{208}Pb , ^{204}Pb is an only non-radiogenic isotope. Therefore, the ratio of radiogenic to total Pb can be estimated from Pb isotopic ratios. We measured Pb isotopic ratios of the zircon samples using laser-ablation (LA) ICP-MS. A UV 213 nm Nd:YAG laser system (UP-213, New Wave Research) was connected to an ICP-MS (Agilent 7500). The zircon samples were scanned over 800 μm with a beam size of 100 μm at a scan speed of 40 $\mu\text{m/s}$. Considering the zoning structures of the zircon samples, five different regions were measured for one grain of each sample.

We prepared the following Pb compounds as reference materials for XANES analysis: divalent $\text{Pb}(\text{NO}_3)_2$, PbCO_3 , PbSO_4 , PbC_2O_4 , PbCrO_4 , $2\text{PbCO}_3 \cdot \text{Pb}(\text{OH})_2$, PbO , PbTiO_3 , PbZrO_3 and $(\text{CH}_3\text{COO})_2\text{Pb} \cdot 3\text{H}_2\text{O}$, mixed-valent Pb_3O_4 and tetravalent PbO_2 and $(\text{CH}_3\text{COO})_4\text{Pb}$. The powder forms of all reagents (purity >99.9%) were diluted to 1 wt% Pb with boron nitride (BN).

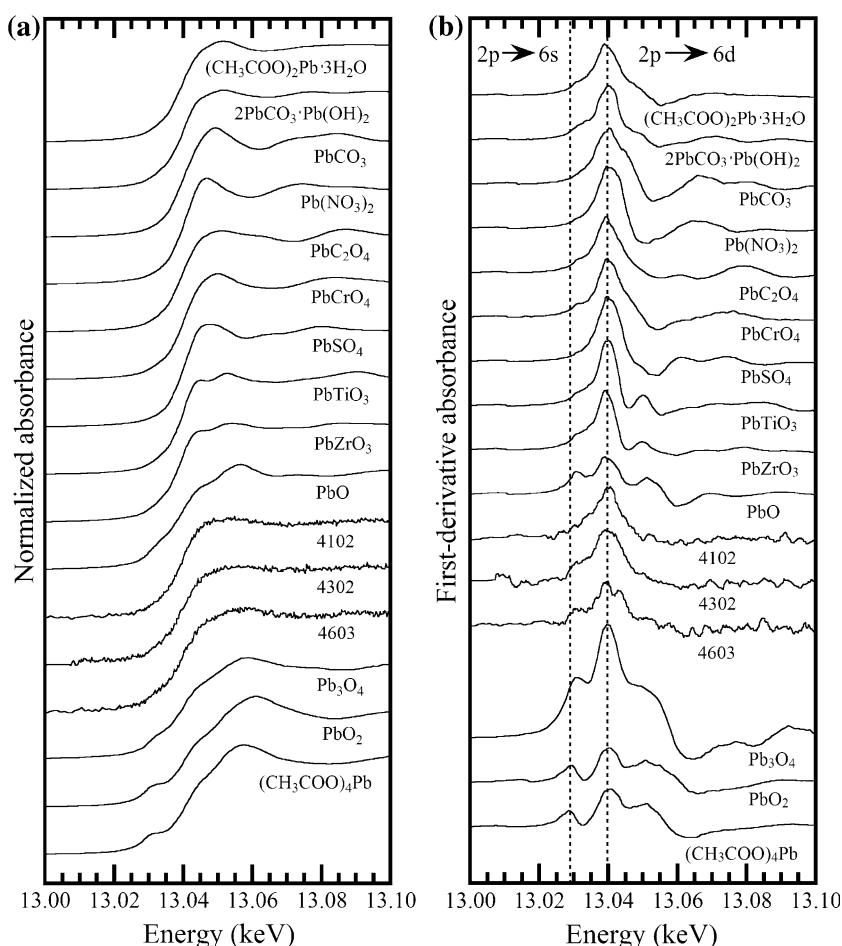
Lead L_{III} -edge (13,040.6 eV) XANES spectra were collected at beamline 12C in Photon Factory, KEK (Tsukuba, Japan). The storage ring was operated at 2.5 GeV, with a typical beam current of 450–300 mA in Photon Factory. A broadband synchrotron radiation from the storage ring was monochromatized with a Si (111) double-crystal monochromator to obtain the incident X-ray beam ($1 \times 1 \text{ mm}^2$). The energy resolution (ΔE) of the Si (111) monochromator at the beamline was ~ 3.5 eV around the Pb L_{III} -edge region. Energy calibration was carried out by assigning the absorption maximum of PbO_2 at 13,060.9 eV. The XANES spectra of the reference materials were collected in transmission mode at room temperature, under ambient conditions, while the measurements of the zircon samples were recorded in fluorescence mode. The energy step in the XANES region was 0.25 eV in all the measurements. Using reference samples,

Table 1 U, Th, and radiogenic Pb concentrations and doses of natural zircon samples (Murakami et al. 1991)

Zircon sample	U (ppm)	Th (ppm)	Radiogenic Pb ^a (ppm)	Dose ($\times 10^{15}$ α/mg)
4102	3,210	1,073	298	6.8
4302	2,069	283	181	4.2
4603	900	330	84	1.9

^a Radiogenic Pb was calculated from U and Th concentrations, assuming an average age of 570 Ma (Gottfried et al. 1956)

Fig. 1 Lead L_{III}-edge XANES spectra of zircon and reference materials. **a** normalized and **b** first-derivative absorbance. The first-derivative absorbance of zircon samples was smoothed by averaging three neighboring points



we confirmed that the transmission and fluorescence modes gave consistent results. The fluorescence yields of the reference and zircon samples, each of which was placed at 45° to the incident X-ray beam, were monitored with a 19-element SSD. Dead time correction for the SSD counting was made (Nomura 1998).

Results

The normalized Pb L_{III}-edge XANES spectra for the zircon samples and the reference materials are shown in Figs. 1 and 2. The first-derivative absorbance of the zircon samples was smoothed by averaging three neighboring points (Figs. 1b, 2). Because the edge features are relatively broad in comparison to the sampling interval (0.25 eV), smoothing should not generate any loss of information in the spectra. The main absorption edge due to the electron transition from 2p to 6d is observed for all zircon samples as well as the reference materials at around 13.040 keV (Rao and Wong 1984). Tetravalent Pb species [PbO₂ and

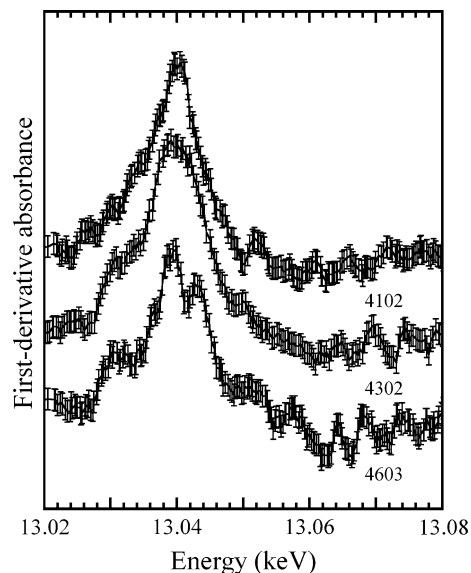


Fig. 2 Comparison of first-derivative absorbance of Pb L_{III}-edge XANES spectra between zircon samples with different amounts of radiation doses. The vertical bars represent statistical error bars

(CH₃COO)₄Pb] with the electronic configuration [Xe]4f¹⁴5d¹⁰6s⁰ show a distinct pre-edge at 13.029 keV due to the electron transition from 2p to 6s, as is clearly observed in the first-derivative absorbance (Fig. 1b) (Rao and Wong 1984; Bargar et al. 1997; Takahashi et al. 2007a). Such transition is not observed for most Pb(II) compounds with [Xe]4f¹⁴5d¹⁰6s² configuration, although PbO indicates the pre-edge at 13.031 keV as a shoulder because of the electron transition from 2p to an energy level produced by the hybridization of the Pb 6s, 6p, and 6d orbitals in PbO (Rao and Wong 1984). Pb₃O₄ also shows 2p → 6s transition around 13.031 keV due to the presence of Pb(IV) in the compound, similar to that of PbO₂ (Gabuda et al. 2005).

Sample 4102 does not exhibit a shoulder at around 13.029 keV in its XANES spectrum (Figs. 1b, 2). The results clearly show that Pb(II) is the main Pb species in the zircon, because the pre-edge feature of 2p → 6s transition is not observed in the XANES spectra of sample 4102. Similar results were obtained for samples 4302 and 4603. However, the samples showed weak peaks at 13.031 keV in the first-derivative, which should be compared to the shoulders in the spectra of PbO, Pb₃O₄, PbO₂, and (CH₃COO)₄Pb (Figs. 1b, 2). The results can be explained by (1) the existence Pb(IV) and/or (2) the hybridization of Pb(II) in the zircon samples. Thus, the pre-edge features of samples 4302 and 4603 suggest a possibility that some Pb are tetravalent.

The results of Pb isotopic ratios by LA-ICP-MS are listed in Table 2. The maximum and minimum values of measurements for five regions within each sample are shown with one standard deviation, respectively. The maximum and minimum values indicate that the Pb isotopic compositions of the zircon samples are fairly heterogeneous, possibly due to the zoning structure. The contribution of common Pb to total Pb was estimated to be <1% (radiogenic/total >0.99) for all the zircon samples even from the minimum values showing the largest contributions of common Pb. Therefore, we can regard almost all Pb in the zircon samples as radiogenic one. The analysis of the Pb isotopic compositions confirmed that radiogenic Pb is divalent in sample 4102 because Pb(II) is the

predominant species (Figs. 1, 2). Similarly, samples 4302 and 4603 contains radiogenic Pb(II), and radiogenic Pb(IV) may also exist in samples 4302 and 4603, as suggested by the shoulder observed at around 13.031 keV in Figs. 1b and 2. We will ignore the presence of common Pb for the further discussion.

Discussion

It has been considered that tetravalent U and Th are located at the Zr sites in zircon (e.g. Ewing et al. 1995; Saaddoune and de Leeuw 2009). Farges and Calas (1991) suggested that Th is eightfold coordinated in metamict zircon using EXAFS. They also observed sixfold coordinated U(IV) in the metamict zircon. However, the location of U and Th has not been precisely characterized in the metamict zircon. Although radiogenic Pb is produced by the radioactive decay of tetravalent U and Th, the successive decay processes may preclude the conservation of electrons around the nucleus because of the numerous intermediate decay products, including an inert gas, Rn (Watson et al. 1997). Hence Watson et al. (1997) considered that there was no reason to expect that radiogenic Pb was tetravalent in zircon. In surface environments, Pb(II) is not easily oxidized to Pb(IV) because even the strong oxidizing agent δMnO₂ does not oxidize Pb(II) (Takahashi et al. 2007a). Consequently, the conclusion that radiogenic Pb is divalent in natural zircon is reasonable, although Pb(II) does not seem to be compatible with the zircon crystal structures as discussed below. In contrast, Kramers et al. (2009) argued that tetravalent state in radiogenic Pb could be produced by the radioactive decays of U and Th, which supports the possibility that some Pb are tetravalent in samples 4302 and 4603 with lower doses. In addition, they suggested that radiogenic Pb(IV) was maintained through geological time in the highly oxidizing environment created by the radioactive decays. However, this seems to be inconsistent with the fact that radiogenic Pb is divalent in sample 4102 with the highest dose (Figs. 1, 2). Further studies are required to understand the low or no content of radiogenic Pb(IV) in highly dosed zircon.

Table 2 Pb isotopic ratios of natural zircon samples

Zircon sample	²⁰⁶ Pb/ ²⁰⁴ Pb	²⁰⁷ Pb/ ²⁰⁴ Pb	²⁰⁸ Pb/ ²⁰⁴ Pb	Radio/tot
4102	Max 8,340 ± 1,275	Max 494 ± 92	Max 775 ± 143	Max 0.993 ± 0.001
	Min 5,443 ± 1,157	Min 328 ± 90	Min 489 ± 100	Min 0.989 ± 0.002
4302	Max 21,860 ± 4,890	Max 1,339 ± 367	Max 844 ± 480	Max 0.997 ± 0.001
	Min 13,940 ± 4,152	Min 785 ± 96	Min 478 ± 118	Min 0.995 ± 0.001
4603	Max 31,180 ± 5,245	Max 1,807 ± 298	Max 2,113 ± 604	Max 0.998 ± 0.001
	Min 5,728 ± 891	Min 367 ± 125	Min 419 ± 90	Min 0.989 ± 0.002

A XANES spectrum reflects the electronic structure of a target atom. The electronic structure of the target atom is related to coordination environments. Therefore, Pb L_{III}-edge XANES spectrum is sensitive to the Pb(II) first-shell coordination environment (Rao and Wong 1984; Bargar et al. 1997). This is recognized by comparing the ionic species of Pb(NO₃)₂ with the covalent one of PbO (Fig. 1) (Rao and Wong 1984; Bargar et al. 1997). The XANES spectra of the zircon samples are different from those of the reference materials (Fig. 1). Hence, it is inferred that the local coordination structures of radiogenic Pb in the zircon samples are different from those of the reference materials.

The average Pb–O distance in the tetravalent compound of PbO₂ is 2.16 Å in sixfold coordination (D'Antonio and Santoro 1980). In the case of Pb(II) the average distances of neighboring O from Pb in PbTiO₃ is 2.66 Å in eightfold coordination (Glazer and Mabud 1978). The average Zr–O distance in zircon is 2.19 Å in eightfold coordination (Robinson et al. 1971). If we assume that radiogenic Pb(II) substitutes for the Zr site, the Pb–O distance may be ~0.45 Å longer than the Zr–O distance in zircon. This large difference suggests that distortion can occur around radiogenic Pb if it occupies the Zr site. The crystal-chemical examination indicates that radiogenic Pb(II) is incompatible with the Zr site although part of the Pb(II) might occupy the Zr site.

Conclusions

We recorded XANES spectra to determine the oxidation state of radiogenic Pb in three natural zircon samples with different radiation doses. Our results show that radiogenic Pb is divalent in the zircon sample with the highest radiation dose. In contrast, the XANES data of the zircon samples with lower radiation doses suggest that a part of Pb may be tetravalent. In any case, radiogenic Pb(II) is present in all the zircon samples.

Acknowledgments The Sri Lankan zircon samples were kindly provided by Prof. R. C. Ewing. We appreciate the constructive reviews by two anonymous reviewers. We likewise thank Dr. M. Matsui for his editorial management. This work was supported by a grant from the Japan Society for the Promotion of Science (JSPS) Research Fellowships for Young Scientists. It was performed with the approval of Photon Factory, KEK (Proposal No. 2007G669 and 2007G670).

References

- Bargar JR, Brown GE Jr, Parks GA (1997) Surface complexation of Pb(II) at oxide–water interfaces: I. XAFS and bond-valence determination of mononuclear and polynuclear Pb(II) sorption products on aluminum oxides. *Geochim Cosmochim Acta* 61:2617–2637
- D'Antonio P, Santoro A (1980) Powder neutron diffraction study of chemically prepared β -lead dioxide. *Acta Crystallogr B* 36:2394–2397
- Davis DW, Krogh TE (2000) Preferential dissolution of ²³⁴U and radiogenic Pb from α -recoil-damaged sites in zircon: implications for thermal histories and Pb isotopic fractionation in the near surface environment. *Chem Geol* 172:41–58
- Ewing RC, Lutze W, Weber WJ (1995) Zircon: a host-phase for the disposal of weapons plutonium. *J Mater Res* 10:243–246
- Farges F, Calas G (1991) Structural analysis of radiation damage in zircon and thorite: an X-ray absorption spectroscopic study. *Am Mineral* 76:60–73
- Faure G (1986) The U, Th–Pb methods of dating. In: *Principles of isotope geology*, 2nd edn. Wiley, New York, pp 282–308
- Gabuda SP, Kozlova SG, Panov VV, Erenburg SB, Bausk NV (2005) XANES Pb L_{III} spectra of mixed-valence compound: minium, Pb₃O₄. *Nucl Instrum Methods A* 543:184–187
- Glazer AM, Mabud SA (1978) Powder profile refinement of lead zirconate titanate at several temperatures. II. Pure PbTiO₃. *Acta Crystallogr B* 34:1065–1070
- Gottfried D, Senftle FE, Waring CL (1956) Age determination of zircon crystals from Ceylon. *Am Mineral* 41:157–161
- Kelley SD, Newville MG, Cheng L, Kemner KM, Sutton SR, Fenter P, Sturchio NC, Spötl C (2003) Uranyl incorporation in natural calcite. *Environ Sci Technol* 37:1284–1287
- Kramers J, Frei R, Newville M, Kober B, Villa I (2009) On the valency state of radiogenic lead in zircon and its consequences. *Chem Geol* 261:4–11
- Meldrum A, Zinkle SJ, Boatner LA, Ewing RC (1998) A transient liquid-like phase in the displacement cascades of zircon, hafnium and thorite. *Nature* 395:56–58
- Murakami T, Chakoumakos BC, Ewing RC, Lumpkin GR, Weber WJ (1991) Alpha-decay event damage in zircon. *Am Mineral* 76:1510–1532
- Nomura M (1998) Dead-time correction of a multi-element SSD for fluorescent XAFS. *J Synchrotron Radiat* 5:851–853
- Rao KJ, Wong J (1984) A XANES investigation of the bonding of divalent lead in solids. *J Chem Phys* 81:4832–4843
- Reeder RJ, Lamble GM, Northrup PA (1999) XAFS study of the coordination and local relaxation around Co²⁺, Zn²⁺, Pb²⁺, and Ba²⁺ trace elements in calcite. *Am Mineral* 84:1049–1060
- Robinson K, Gibbs GV, Ribbe RH (1971) The structure of zircon: a comparison with garnet. *Am Mineral* 56:782–789
- Saaddoune I, de Leeuw NH (2009) A computer simulation study of the accommodation and diffusion of He in uranium- and plutonium-doped zircon (ZrSiO₄). *Geochim Cosmochim Acta* 73:3880–3893
- Shannon RD (1976) Revised effective ionic radii and systematic studies of interatomic distances in halides and chalcogenides. *Acta Crystallogr A* 32:751–767
- Takahashi Y, Manceau A, Geoffroy N, Marcus MA, Usui A (2007a) Chemical and structural control of the partitioning of Co, Ce and Pb in marine ferromanganese oxides. *Geochim Cosmochim Acta* 71:984–1008
- Takahashi Y, Uruga T, Suzuki K, Tanida H, Terada Y, Hattori KH (2007b) An atomic level study of rhenium and radiogenic osmium in molybdenite. *Geochim Cosmochim Acta* 71:5180–5190
- Utsunomiya S, Palenik CS, Valley JW, Cavosie AJ, Wilde SA, Ewing RC (2004) Nanoscale occurrence of Pb in an Archean zircon. *Geochim Cosmochim Acta* 68:4679–4686
- Utsunomiya S, Valley JW, Cavosie AJ, Wilde SA, Ewing RC (2007) Radiation damage and alteration of zircon from a 3.3 Ga porphyritic granite from the Jack Hills, Western Australia. *Chem Geol* 236:92–111

Watson EB, Cherniak DJ, Hanchar JM, Harrison TM, Wark DA (1997) The incorporation of Pb into zircon. *Chem Geol* 141:19–31

Zhang M, Boatner LA, Salje EKH, Ewing RC, Daniel P, Weber WJ, Zhang Y, Farnan I (2008) Micro-Raman and micro-infrared

spectroscopic studies of Pb- and Au-irradiated ZrSiO₄: optical properties, structural damage, and amorphization. *Phys Rev B* 77:144110